



The Effect of Work Hardening on the Structure and Hardness of Hadfield Steel

D. Bańkowski * , P.S. Młynarczyk , W. Depczyński , K.C. Bolanowski 
Kielce University of Technology, Poland

* Corresponding author: E-mail address: damianbankowski1@gmail.com

Received 23.08.2023; accepted in revised form 19.12.2023; available online 15.02.2024

Abstract

The article aims to characterize Hadfield steel by analyzing its chemical composition, mechanical properties, and microstructure. The study focused on the twinning-induced work hardening of the alloy, which led to an increase in its hardness. The experimental data show that the material hardness at the surface improved considerably after solution heat treatment and work hardening, reaching more than 750 HV. By contrast, the hardness of the material core in the supersaturated condition was about 225 HV. The chemical and phase compositions of the material at the surface were compared with those of the core. The microstructural analysis of the steel revealed characteristic decarburization of the surface layer after solution heat treatment. The article also describes the effects of heat treatment on the properties and microstructure of Hadfield steel. The volumetric (qualitative) analysis of the computed tomography (CT) data of Hadfield steel subjected to heavy dynamic loading helped detect internal flaws, assess the material quality, and potentially prevent the structural failure or damage of the element tested.

Keywords: Manganese steel, Hardness, Modified Hadfield steel, Solution heat treatment, Computed tomography

1. Introduction

A characteristic feature of Hadfield steel is its ability to strain hardening. The alloy exhibits high mechanical properties, especially high resistance to abrasion [1]. Hadfield steel is also known as manganese steel because of a high content of this element.

When the material is in a supersaturated state, an austenitic microstructure (austenite matrix) forms. Under high stress or impact loads, it strengthens [1-6]. The high hardness and high resistance to abrasion are due to the formation of a twinned structure [5].

Hadfield steel has been known to be resistant to abrasion for over 140 years. It was named after its inventor, Robert Hadfield. The material contains 1.1–1.3% C, 0.3–1.0% Si, and 11–13 % Mn [1, 6-9]; the other alloying elements are generally treated as impurities or trace elements resulting from the modification of

liquid metal before it is poured into a mold. The carbon-to-manganese ratio is typically about 1:10.

The microstructural analysis of the as-cast manganese steel reveals austenite and needle-like carbides [10]. The presence of non-metallic inclusions and carbides is not beneficial from the performance point of view as these will be responsible for lower ductility of the alloy. From the literature on the subject [6], it is evident that carbide precipitates occurring along the grain boundaries may cause a tenfold decrease in the impact strength of the material. Solution heat treatment is thus essential to obtain a purely austenitic structure.

The performance of Hadfield steel can be improved by work hardening [10, 11], being a result of microtwinning. Deformation twinning is due to deformations in the surface layer. The deformations arise from stresses above the proportional, elastic and plastic limits. The original crystal and its twin are like an object and its reflection in a flat mirror, respectively. It should be noted, however, that a crystal may undergo repeated or multiple



twinning [12]. Deformation twinning can be defined as rapid sliding displacements of atoms occurring in a small area surrounded by twin boundaries. Twins strengthen the crystal, increasing its tensile strength, R_m , yield strength, R_e , and brittleness. In [10], it is indicated that twins hinder the movement of dislocations; this however, contributes to the formation of crack nuclei at the boundaries where dislocations accumulate. The hardness of Hadfield steel vary between 190 and 220 HB; it can increase even twice to over 500 HB after work hardening [10]. One of the studies on the mechanical behavior of Hadfield steel [13] shows that when the surface layer is exposed to repeated heavy dynamic loading, its hardness reaches approx. 850 HV0.1.

Figure 1 shows the phase diagram for the Fe-Mn-C alloy with a manganese content of 13%.

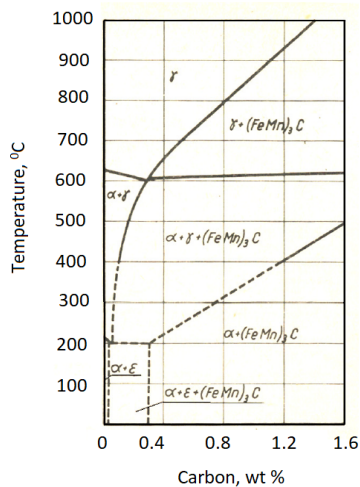


Fig. 1 Vertical section of the Fe-Mn-C alloy phase diagram at 13% Mn [14]

Hadfield steel retains high hardness at elevated temperatures (300 – 400 °C) [14]. Before it can be machined, it needs to be subjected to isothermal annealing at 600 °C [14]. The annealing process results in the precipitation of carbides from the austenite and partial pearlite transformation [14]. A similar effect, i.e., a reduction in the material hardness and its softening, can be achieved by slow cooling or heating the cast alloy to the lowest austenite transformation temperature.

The addition of chromium and vanadium to Hadfield steel causes the precipitation of carbides with a low free energy throughout the austenite, including the matrix; this phenomenon contributes to higher hardness and toughness, and, consequently, higher resistance to abrasion of the austenite matrix [15, 16].

The strengthening of the material can also be obtained by isothermal annealing at a temperature of about 600 °C, which leads to the precipitation of carbides from the austenite followed by partial pearlitic transformation [14].

Some researchers [16-21] aimed to fabricate alloys super resistant to abrasion; the materials contained a high percentage of networks of carbides at the austenite grain boundaries, like in Hadfield steel. Similar observations have been made for white cast iron (with a sub-eutectic composition) exposed to a temperature higher than the eutectoid transformation temperature.

Some researchers, for example, [13] claim that the resistance to abrasion of Hadfield steel with a hardened surface layer is similar to or even higher than those of various quenched bearing steels.

The research described in [22] reveals that, instead of heat treatment, which is an expensive and time-consuming process, Hadfield steel can be strengthened by adding a modifying agent, e.g., cerium, yttrium, silicon, or magnesium, to the material in the liquid state. These elements have the capability to form oxides and sulfides. The pseudo-eutectic phase that forms during solidification consists of austenite and carbides between the austenite dendrites.

The benefits of ladle treatment over traditional heat treatment for Hadfield steel are discussed in [15]. The effects of ladle treatment to strengthen the alloy were reported to be twice as high as those of the conventional heat treatment process. The phenomena behind the increase in the work hardening properties of the material involve the formation of a new eutectic phase, i.e., an austenite phase enriched by carbon and manganese solutes [15].

Another article on the subject [23] investigates how the different contents of Mg affect the behavior of proeutectoid needle-shaped carbides in Hadfield steel. The study involved determining the size of the austenite grains as well as the mechanical properties of the alloy, i.e., hardness (HV), resistance to abrasion, and impact strength. The experimental data revealed that Mg added to Hadfield steel was responsible for the refinement of the austenite grains and the improvement in the material properties, especially resistance to abrasion, hardness (HV), and impact strength (up to 250%) [23].

In [24], the research involved improving the mechanical properties of as-cast Hadfield steel by adding SiZr38 as an inoculant; the ultimate tensile strength and the yield strength of the material increased by 8% and 4%, respectively. Even a small amount of SiZr38 (0.02% wt.) was able to modify the alloy; the result was a decrease in both the grain diameter and the secondary dendrite arm spacing (SDAS), which led to approximately 34% higher resistance to abrasion of as-cast Hadfield steel [24].

The high ductility and good wear resistance of Hadfield steel alloys, achieved by work hardening make the materials increasingly popular. They are suitable for elements operating under abrasive wear and dynamic loading conditions, for example, mining teeth, mine rails, railroad switches, and strongboxes [13, 25-28].

The aim of the study was to analyze the influence of plastic and elastic deformations on the behavior of Hadfield steel under dynamic loading at a constant amplitude of deformations. The novelty of the research was to relate the deformation twinning to the occurrence of crack nuclei using computed tomography data.

2. Materials and methods

The effects of work hardening were studied using railroad switch elements subjected to dynamic loading. The computed tomography scans were carried out for an element of a railroad switch containing a crack.

The composition of the material determined with a Bruker Q8 Magellan spark emission spectrometer, is shown in Table 1.

Table 1.

Chemical composition of Hadfield steel, wt. %

C	Si	Mn	P	Cr	Ni	Mo	Ti	V	Nb	Fe
1.1	0.5	11.8	0.03	0.14	0.04	0.02	0.06	0.056	0.007	rest
1.1	0.4	11.4	0.035	0.20	0.07	0.01	0.04	0.04	0.01	rest

The microstructural examinations were conducted by means of a Nikon Eclipse MA200 optical microscope equipped with NIS 4.20-Elements Viewer imaging software.

The hardness of the Hadfield steel plates was measured at a load of 5 kG (49.03 N) with an HPO-10 hardness tester made by Werkstoffprüfmaschinen.

The phase composition was determined using a Bruker D8 X-ray diffractometer, fitted with a cobalt anode.

Computed tomography (CT) scanning was performed with a Nikon M2 LES system. The 450kV/450W microfocus X-ray source was selected for the tests. A VAREX XRD 1611 detector was employed. The scanning results were analyzed with the CT Agent software, while VGStudio MAX 2022.4.1 was used for the data visualization.

3. Results and discussion

As-cast manganese steel does not exhibit any special properties. The literature indicates that the material is not resistant to abrasion if a layer of work hardened (twinned) austenite has not formed. Generally, at a slow cooling rate, manganese steel with

The analysis was carried out twice.

1.1-1.3% C has a complex structure (austenite, pearlite, and carbides). [10].

Figure 2 shows the microstructure of the surface layer of as-cast Hadfield steel.

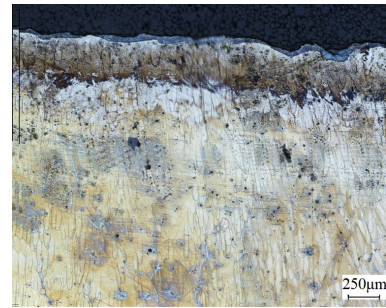


Fig. 2. Microstructure of the surface layer of the as-cast Hadfield steel. (magnification 50x)

For large-size castings, a small rate of cooling after crystallization contributes to the precipitation of carbides mainly at the grain boundaries. Unevenly distributed areas of eutectics and carbide precipitates can be seen in the microphotographs in Figure 3.

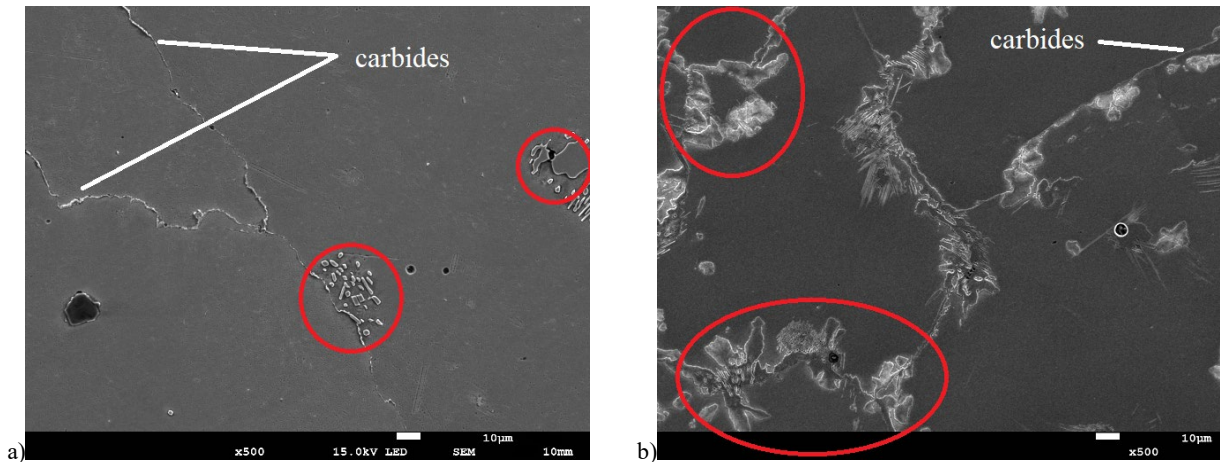


Fig. 3. Microphotographs of as-cast Hadfield steel with a) precipitates of carbides and local eutectics at the grain boundaries b) eutectics (carbides) at the grain boundaries

Depending on the crystallization conditions, carbide precipitates may differ in shape, size, and number. The addition of chromium leads to the formation of the austenite matrix with numerous needle-shaped carbide precipitates and local eutectics at the grain boundaries (Figures 3 a) and b)).

The location of carbides along the boundaries between dendrites is not favorable; under dynamic loading conditions,

cracks may form along the boundaries between the carbide and austenite phases, leading to the material failure. For this reason, casting is frequently followed by heat treatment at a high temperature to dissolve carbides. Rapid cooling ensures that the austenite microstructure remains unchanged in the cast steel.

As-cast Hadfield steel is frequently subjected to solution heat treatment to stabilize the austenite matrix. Solution heat treatment

occurs at a temperature ranging from 1000 °C to 1100 °C, depending on the carbon content, and it is followed by rapid cooling [4] to ‘freeze’ the austenite microstructure. The presence of the needle-shaped carbides makes it necessary to extend the

heat treatment time to ensure that the carbides dissolve into the austenite matrix [4]. Figure 4 shows the microstructure of Hadfield steel after 30-minute solution heat treatment at 1050 °C followed by cooling in water.

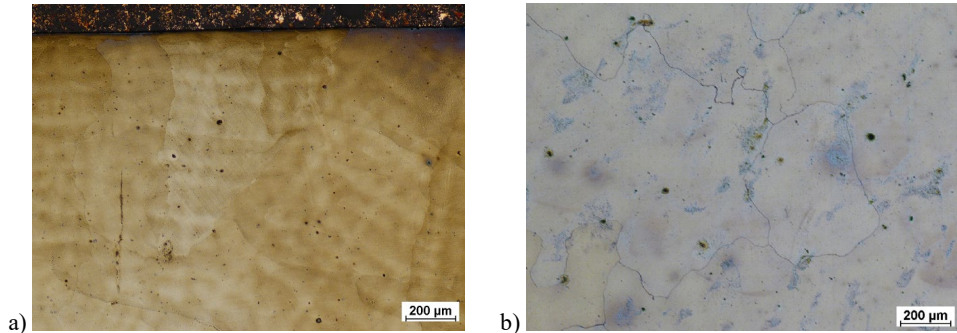


Fig. 4. Microimages of Hadfield steel after solution heat treatment (magnification 50x), a) dendritic structure at the surface, b) grain boundaries and material discontinuities in the core

As can be seen from Figure 4 a), the material has a dendritic structure with inclusions, impurities and voids. In Figure 4 b), the grain boundaries, impurities as well as voids and pores are clearly visible.

To confirm the literature data, the hardness of the alloy was measured before the material was work hardening. It ranged about 225 HV5. To confirm the beneficial effects of work hardening, the hardness of Hadfield steel was determined using an element of a railroad switch, which while used had been exposed to large dynamic loading. The microstructure of the material is shown in Figure 5. The indentations left by the hardness tester are depicted in Figure 6.

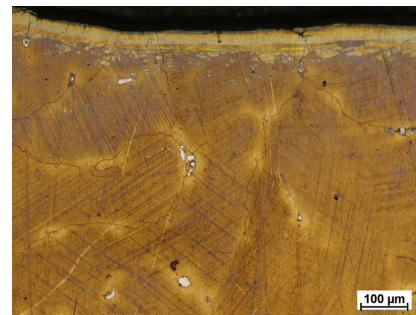


Fig. 5. Hadfield steel after work hardening

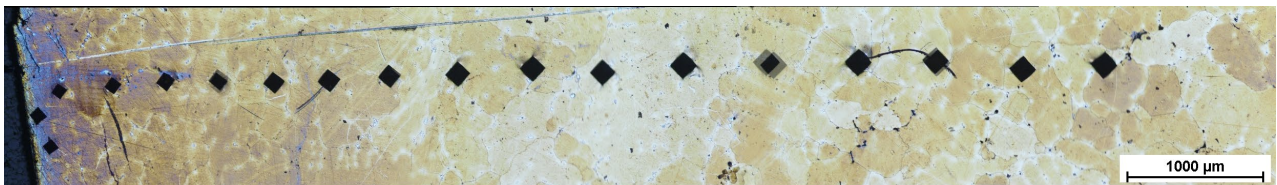


Fig. 6. Indentations left after the hardness test

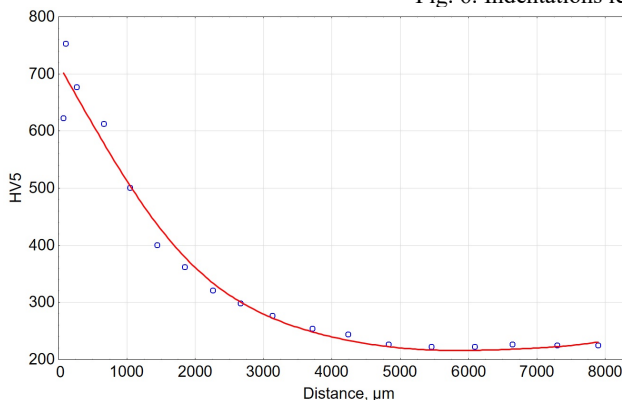


Fig. 7. Hardness vs. distance from the surface for work-hardened Hadfield steel

The hardness data obtained with an HPO-10 hardness tester by applying a force of 5 kG (49.03 N) are plotted in Figure 7.

Changes in the grain size and the material microstructure, which can be observed at different depths, were due to the crystallization of steel.

The measurement results confirm that at the surface the hardness of Hadfield steel is higher, reaching about 750 HV5. From the hardness data and the diagram in Figure 7, we can conclude that the hardness gradually decreases and stabilizes at a depth of about 5 mm from the work-hardened surface.

The microscopic examination data also confirm the occurrence of deformation twinning being a result of the indentations. When viewed by polarized light microscopy (Figure 8), the material features characteristic deformation twinning lines close to the indentation edges.

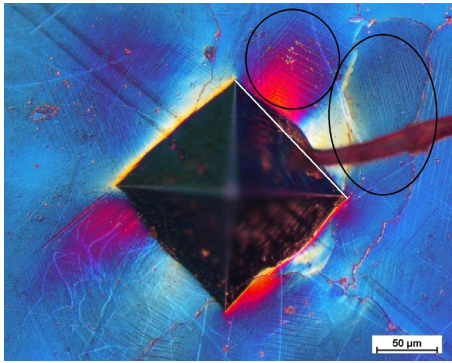


Fig. 8. Microphotograph showing an indentation left after a Vickers hardness test

Surface deformation can be observed in the adjacent areas (the black ellipses) in Figure 8. From the indentation left after the Vickers hardness test (Figure 8), it is evident that the edges are curved when compared with a straight line (in white).

Figure 9 shows a micrograph of the surface layer of Hadfield steel after solution heat treatment. In Figure 9 (unlike in Figures 2, 4 a), and 5) the decarburization zone is clearly visible; the characteristic ferrite occurs only in the surface layer. The results of the microscopic analysis were confirmed by the chemical composition and qualitative analysis data. The surface layer was about 500 μm in thickness (Figure 9).



Fig. 9. Microphotograph showing Hadfield steel after solution heat treatment

The chemical composition analysis and the qualitative analysis of the phase composition were conducted at the surface of the as-cast material and in the core after cutting the alloy by abrasive water jet (AWJ) cutting. Table 2 shows the chemical composition of the steel alloy at the surface and in the core after solution heat treatment.

Figure 10 b) illustrates a diffractogram of the material at the surface while Figure 10 a) shows a diffractogram of the core of the as-cast alloy (cross-section obtained by AWJ).

Table 2.

Chemical composition of Hadfield steel after solution heat treatment: at the surface and in the core, wt. %.

	C	Si	Mn	P	Cr	Ni	Mo	Ti	W	Ni	Fe
surface area	0.2	0.5	12.1	0.04	0.15	0.05	0.02	0.07	0.065	0.009	rest
core	1.1	0.5	11.8	0.03	0.14	0.04	0.02	0.06	0.056	0.007	rest

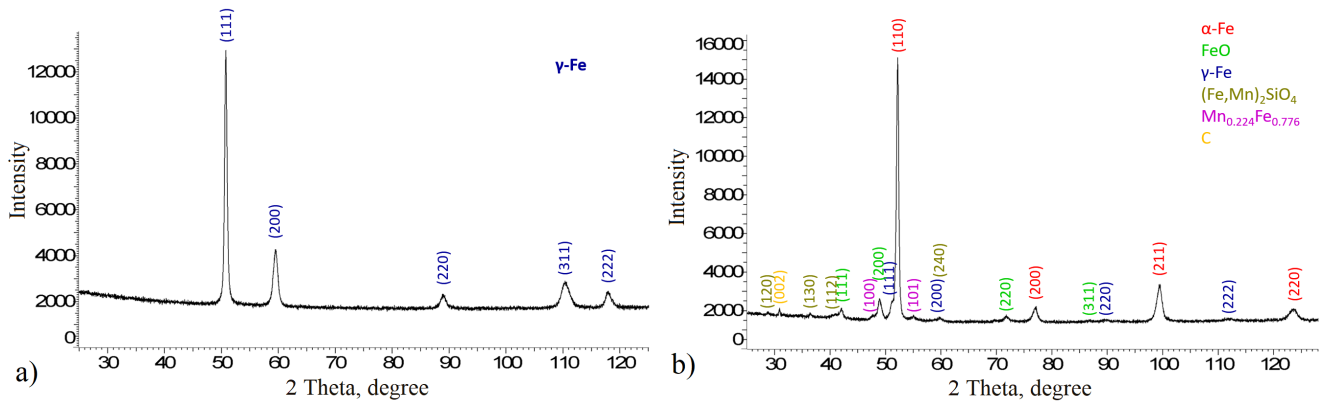


Fig. 10. Diffractograms of Hadfield steel after solution heat treatment: a) the core b) the surface layer

From the diffractograms in Figures 10 a) and b), it can be concluded that compounds rich in silicon (Si) may form at the surface when Hadfield steel is cast into molds containing quartz sand and other minerals. As the measuring point was located at the casting surface, the occurrence of graphite was probably due to the contamination from the mold.

The analysis of the chemical and phase compositions of the alloy confirms that the carbon content decreased at the surface. Annealing at 1000–1100 °C, i.e., a temperature at which steel

reaches solution heat treatment, led to the decarburization of the surface layer to a depth of 0.5–1.5 mm. Consequently, the stabilization of ferrite in this layer took place at a temperature of less than 300–500 °C, depending on the carbon content (Figure 1). This indicates how important the role of carbon is in the stabilization of austenite.

Annealing at a temperature of about 600–650 °C is commonly used to improve the material machinability. After machining, however, solution heat treatment was repeated to restore the

original microstructure, i.e., the austenite matrix without carbide precipitates, offering favorable operating conditions.

Carbides are badly located along the boundaries between the dendrites. Solution heat treatment in an atmosphere rich in oxygen causes decarburization and the formation of oxides (wüstite - FeO).

The deformation twinning, which hinders the movement of dislocations, may be the cause of crack nuclei formation at the boundaries where the dislocations accumulate [10]. Figure 11 displays a micrograph of work hardened Hadfield steel (railroad switch element) with numerous cracks, attributable to the accumulation of dislocations at the twin boundaries. The composition of the material (railroad switch element) subjected to dynamic loading was determined using volumetric analysis.

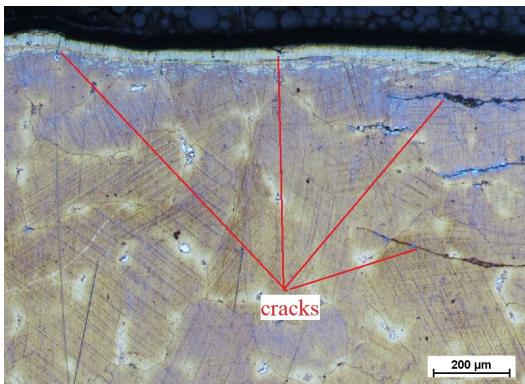


Fig.11. Microphotograph of work hardened Hadfield steel

The volumetric analysis of Hadfield steel was performed to show that uncontrolled work hardening might have a negative effect. Figure 12 shows three mutually perpendicular cross-sections and a 3D rectangular model of Hadfield steel.

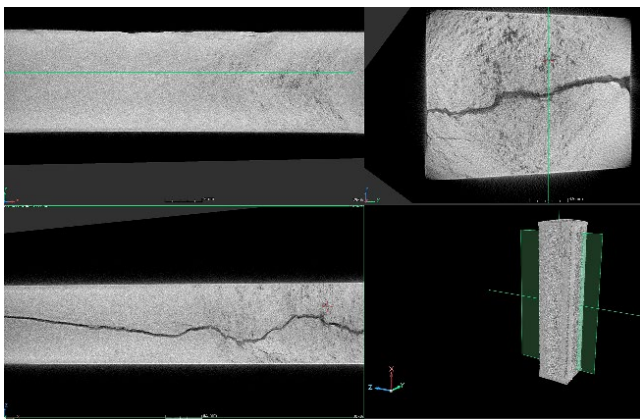


Fig. 12. 2D and 3D visualization of segmented images (VG Studio)

Figure 12 shows areas of lower density in different cross-sections. The occurrence of undesirable cracks, pores, voids, and other flaws was due to the work hardening and of the casting process. Accumulated flaws are often responsible for element cracking under operating conditions.

Computed tomography is an indispensable tool for volumetric analysis. Computed tomography scan provides a 3D image of the object viewed based on hundreds of 2D radiographs. Figure 13 displays internal flaws, including small near surface cracks, pores, and voids, reconstructed using computed tomography. As can be seen in Figure 13, the flaws differed in volume.

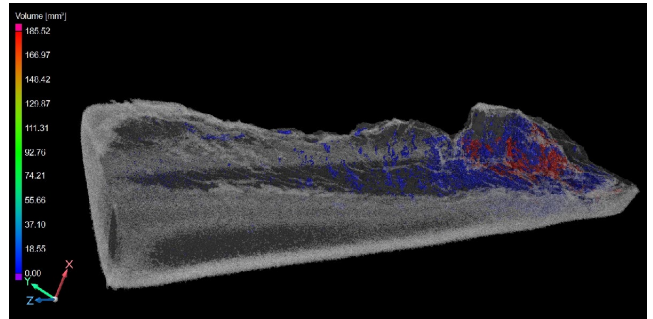


Fig. 13. The 3D Computed tomographic reconstruction of the porosity analysis of the fracture surface of Hadfield steel, with marked cracks

The computed tomography reconstruction of an element of a railroad switch, cast from Hadfield steel, which failed due to a crack, confirms the occurrence of numerous internal casting flaws.

4. Conclusions

As-cast Hadfield steel was reported to have a ferritic microstructure with carbide precipitates along the grain boundaries; their shapes, sizes, and number were dependent on the casting geometry and crystallization conditions, especially the cooling rate.

Hadfield steel can be hardened by solution heat treatment and work hardening. Annealing performed at a temperature of 1000-1100 °C followed by rapid cooling retains the austenite structure. When the material is work hardened by deformation twinning, the hardness increases to more than 750 HV.

An increase in work hardening may lead to the formation of numerous crack nuclei, which, under dynamic loading conditions, may be responsible for crack propagation and, consequently, the material failure.

Solution heat treatment of as-cast Hadfield steel results in the decarburization at the surface. Changes can be observed to a depth of 0.5–1.5 mm.

Computed tomography helps assess the quality of cast elements. It is crucial that the casting process should be properly designed for Hadfield steel to prevent the occurrence of typical flaws such as voids and pores.

References

- [1] Kalandyk, B., Tęcza, G., Zapała, R., Sobula, S. (2015). Cast high-manganese steel – the effect of microstructure on

- abrasive wear behaviour in miller test. *Archives of Foundry Engineering*. 15(2), 35-38. DOI: 10.1515/afe-2015-0033.
- [2] Bartlett, L.N. & Avila, B.R. (2016). Grain refinement in lightweight advanced high-strength steel castings. *International Journal of Metalcasting*. 10, 401-420, DOI: 10.1007/s40962-016-0048-0.
- [3] Guzman Fernandes, P.E. & Arruda, Santos, L. (2020). Effect of titanium and nitrogen inoculation on the microstructure, mechanical properties and abrasive wear resistance of Hadfield Steels. *REM - International Engineering Journal*. 73(5), 77-83. <https://doi.org/10.1590/0370-44672019730023>
- [4] Chen, C., Lv, B., Feng, X., Zhang, F. & Beladi, H. (2018). Strain hardening and nanocrystallization behaviors in Hadfield steel subjected to surface severe plastic deformation. *Materials Science and Engineering: A*. 729, 178-184. DOI:10.1016/j.msea.2018.05.059.
- [5] Chen, C., Zhang, F.C., Wang, F., Liu, H. & Yu, B.D. (2017). Effect of N+Cr alloying on the microstructures and tensile properties of Hadfield steel. *Materials Science & Engineering*. 679, 95-103. DOI:10.1016/j.msea.2016.09.106.
- [6] Bolanowski, K. (2008). Wear of working elements made of Hadfield cast steel under industrial conditions. *Problemy Eksploatacji*. 2, 25-32.
- [7] Tęcza, G., Sobula, S. (2014). Effect of heat treatment on change microstructure of cast high-manganese Hadfield steel with elevated chromium content. *Archives of Foundry Engineering*. 14(3), 67-70.
- [8] Gürol, U., Karadeniz, E., Çoban, O., & Kurnaz, S.C. (2021). Casting properties of ASTM A128 Gr. E1 steel modified with Mn-alloying and titanium ladle treatment. *China Foundry*. 18, 199-206. <https://doi.org/10.1007/s41230-021-1002-1>
- [9] Pribulová, A., Babic, J. & Baricová, D. (2011). Influence of Hadfield's steel chemical composition on its mechanical properties. *Chem. Listy*. 105, 430-432.
- [10] Przybyłowicz, K. (2008). *Iron alloys engineering*. Kielce: Wyd. Politechniki Świętokrzyskiej w Kielcach (in Polish).
- [11] Stradomski, Z. (2001). On the explosive hardening of cast Hadfield steel. *Proceedings of a Conference on Advanced Steel Casting Technologies*. Kraków. 112-122. (in Polish).
- [12] Cullity, B.D. (1964). *Basics of X-ray diffraction*. Warszawa: PWN. (in Polish).
- [13] Bolanowski, K. (2013). The influence of the hardness of the surface layer on the abrasion resistance of Hadfield cast steel. *Problemy Eksploatacji*. 1, 127-139. (in Polish).
- [14] Przybyłowicz, K. (2012). *Metal Science*. Warszawa: WNT. (in Polish).
- [15] El Fawjhry, M.K. (2018). Feasibility of new ladle-treated Hadfield steel for mining purposes. *International Journal of Minerals, Metallurgy and Materials*. 25(3), 300, <https://doi.org/10.1007/s12613-018-1573-z>.
- [16] Subramanyan, D.K., Swansieger, A.E. and Avery, H.S. (1990). Austenitic manganese steels. In *ASM Metals Handbook*. Vol. 1, 10th Ed. (p. 822-840). India: American Society of Metals, India.
- [17] Zykova, A., Popova, N., Kalashnikov, M. & Kurzina, I. (2017). Fine structure and phase composition of Fe-14Mn-1.2C steel: influence of a modified mixture based on refractory metals. *International Journal of Minerals, Metallurgy and Materials*. 24(5), 523-529. DOI: 10.1007/s12613-017-1433-2.
- [18] Vdovin, K.N., Feoktistov, N.A., Gorlenko, D.A. et al. (2019). Modification of High-Manganese Steel Castings with Titanium Carbonitride. *Steel in Translation*. 3, 147-151. <https://doi.org/10.3103/S0967091219030136>.
- [19] Issagulov, A.Z., Akhmetov, A.B., Naboko, Ye.P., Kusainova, G.D. & Kuzhanova, A.A. (2016). The research of modification process of steel Hadfield integrated alloy ferroalumisilicocalcium (Fe-Al-Si-Ca/FASC). *Metallurgija*. 55(3), 333-336.
- [20] Haakonsen, F., Solberg, J.K., Klevan, O. & Van der Eijk, C. (2011). Grain refinement of austenitic manganese steels. In *AISTech - Iron and Steel Technology Conference Proceedings*, 5-6 May 2011 (pp. 763-771). Indianapolis, USA.
- [21] El Fawkhry, M.K. (2021). Modified hadfield steel for castings of high and low gouging applications. *International Journal of Metalcasting*. 15(2), 613-624. <https://doi.org/10.1007/s40962-020-00492-5>.
- [22] El Fawkhry, M.K., Fathy, A.M. and Eissa, M.M. (2015). New energy saving technology for producing Hadfield steel to high gouging applications. *Steel Research International*. 86(3), 223-230. <https://doi.org/10.1002/srin.201300388>.
- [23] El-Fawkhry, M.K., Fathy, A.M., Eissa, M. & El-Faramway, H. (2014). Eliminating heat treatment of Hadfield steel in stress abrasion wear applications. *International Journal of Metalcasting*. 8, 29-36. DOI: 10.1007/BF03355569
- [24] Sobula, S., Kraiński, S. (2021). Effect of SiZr modification on the microstructure and properties of high manganese cast steel. *Archives of Foundry Engineering*. 4, 82-86. ISSN (1897-3310).
- [25] Zambrano, O.A., Tressia, G., Souza, R.M. (2020). Failure analysis of a crossing rail made of Hadfield steel after severe plastic deformation induced by wheel-rail interaction. *Engineering Failure Analysis*. 115, 104621. DOI: doi.org/10.1016/j.engfailanal.2020.104621.
- [26] Wróbel, T., Bartocha, D., Jezierski, J., Kalandyk, B., Sobula, S., Tęcza, G., Kostrzewa, K., Feliks E. High-manganese alloy cast steel in applications for cast elements of railway infrastructure. In *Współpraca 2023: XXIX international scientific conference of Polish, Czech and Slovak foundrymen*, 26-28 April 2023. Niepołomice.
- [27] Młyński, M., Sobula, S., Furgał, G. (2001). Economic aspects of the oxygen-recovery melts of Hadfield cast steel in the Foundry of Metalodlew S.A. *Przegląd Odlewnictwa*. 51(11), 382-384. (in Polish).
- [28] Wróbel, T., Bartocha, D., Jezierski, J., Sobula, S., Kostrzewa K., Feliks E. (2023). High-manganese alloy cast steel used for cast elements of railway infrastructure. *Stal, Metale & Nowe Technologie*. 1-2, 30-34. (in Polish).